Electronic Supplementary Material (ESI) for CrystEngComm.

Supporting Information

A facile one-pot synthesis of Co_2P nanoparticle-encapsulated doped carbon nanotubes as bifunctional electrocatalysts for high-performance rechargeable Zn-air batteries

Qi Shao, Tianjiao Li, Heng-guo Wang*, Yanhui Li, Zhenjun Si and Qian Duan*

School of Materials Science and Engineering, Changchun University of Science and Technology, Changchun 130022, China

Experimental Section

Materials

Phosphonitrilic chloride trimer ($Cl_6N_3P_3$), melamine and cobalt acetylacetonate ($C_{15}H_{21}CoO_6$) were purchased from Aladdin Chemical Reagent Co. Ltd. All materials were used without further purification. De-ionized water was obtained from an ultra-pure purification system.

Characterization

The microstructures of the nanomaterials were observed by scanning electron microscopy (SEM Hitachi S-4800) and transmission electron microscope (TEM) recorded on a Tecnai G2 operating at 200 kV. The crystal phases were evaluated by X-ray diffraction (XRD) patterns recorded on a Rigaku-Dmax 2500 diffractometer with Cu Ka radiation. X-ray photoelectron spectroscopy (XPS) analysis conducted with Thermo SCIENTIFIC ESCALAB 250Xi instrument was used to analyze the composition of the nanomaterials. Raman spectra were collected with a Renishaw 2000 model confocal microscopy Raman spectrometer.

Electrochemical Measurements

All electrochemical measurements were conducted on CS350 electrochemical workstation. The ORR/OER properties were taken on a three-electrode system in the corresponding electrolyte. The working electrode was RDE (5.0 mm in diameter), while the reference electrode was saturated calomel electrode (SCE) and the counter electrode was the graphite rod, respectively.

To prepare the working electrode, 1 mL ethanol containing catalyst (5 mg) and Nafion solution (50 μL) were ultrasonically dispersed to obtain the homogeneous ink. Afterward, 10 μL ink catalyst was dropped onto RDE and then dried at room temperature. The recorded potentials versus SCE were converted to RHE scale based

on the Nernst equation ($E_{RHE}=E_{SCE}+0.241+0.059pH$). As for ORR experiment, the CV tests were acquired in N_2- or O_2-saturated 0.1 M KOH solution with a scan rate of 50 mV s^{-1}. LSV measurements were conducted at different speeds from 400 to 1600 rpm in an O_2-saturated solution with a sweep rate of 10 mV s^{-1} without being *iR*-corrected. According to the LSV curves at the different potentials, the electron transfer number (n) was calculated according to the Koutecky-Levich (K-L) equations.

As for OER experiments, the LSV curves were obtained at a scan rate of 5 mV s^{-1} with being *iR*-corrected in the O_2-saturated 1 M KOH solution. Before all the electrochemical characterizations, the continuous sweep of corresponding voltage range is measured until the steady voltammogram curve is obtained.

The durability tests of the electrocatalysts for OER and ORR were both evaluated using chronoamperometric (i-t) measurement in corresponding solution at a rotation rate of 1600 rpm.

Supplemental Figures

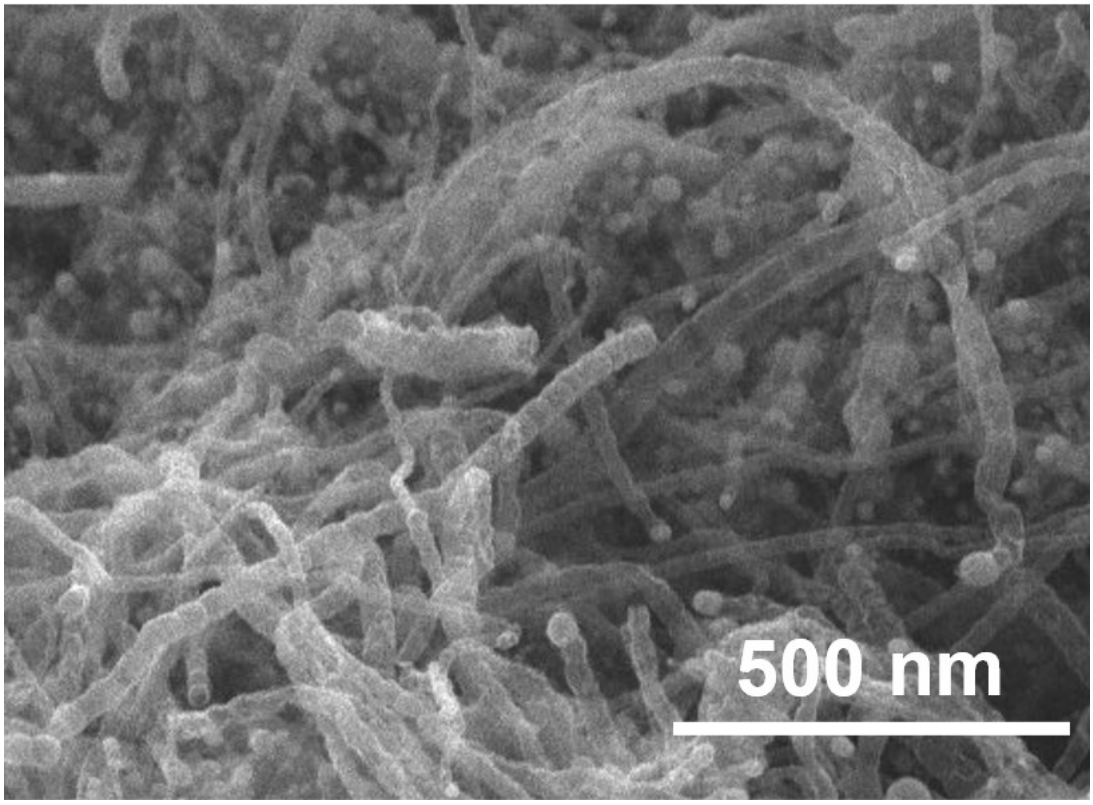

Fig. S1 SEM image of Co_2P@NPCNTs-900.

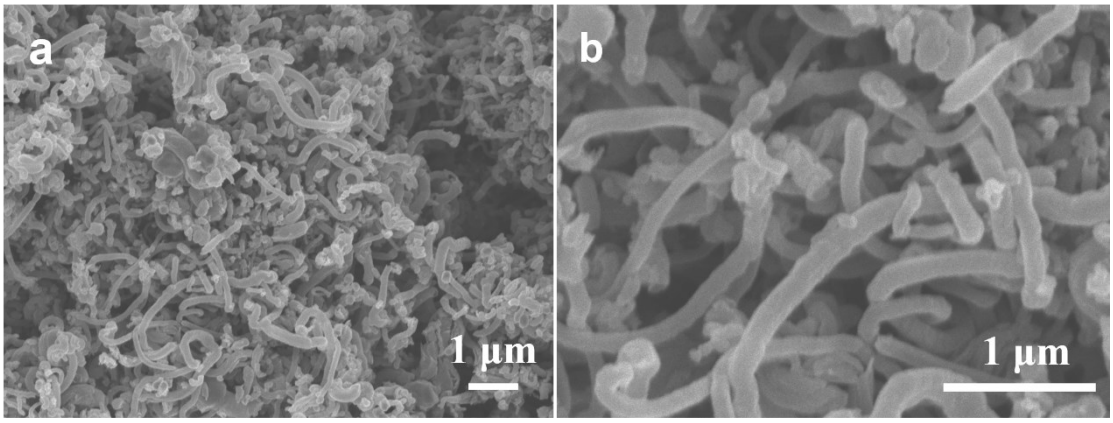

Fig. S2 (a) Low and (b) high-resolution SEM images of Co@NCNTs-900.

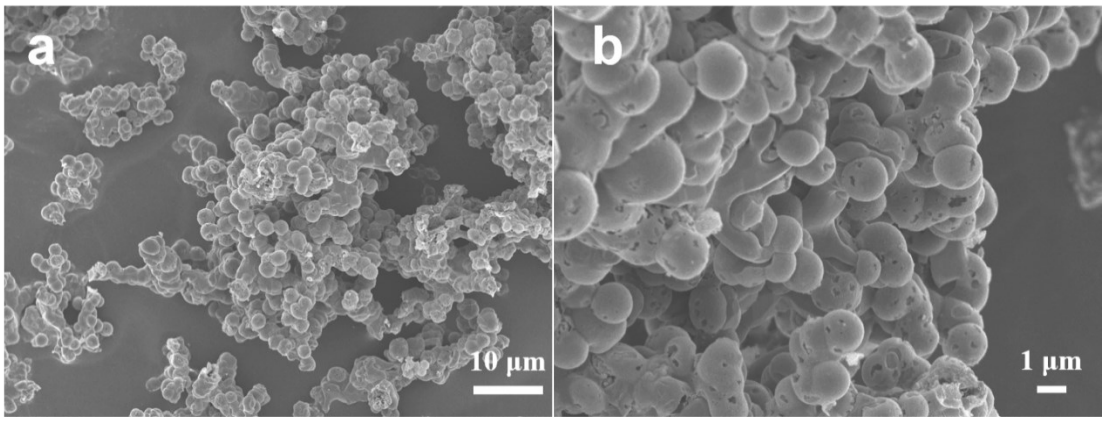

Fig. S3 (a) Low and (b) high-resolution SEM images of Co_2P@NPC-900.

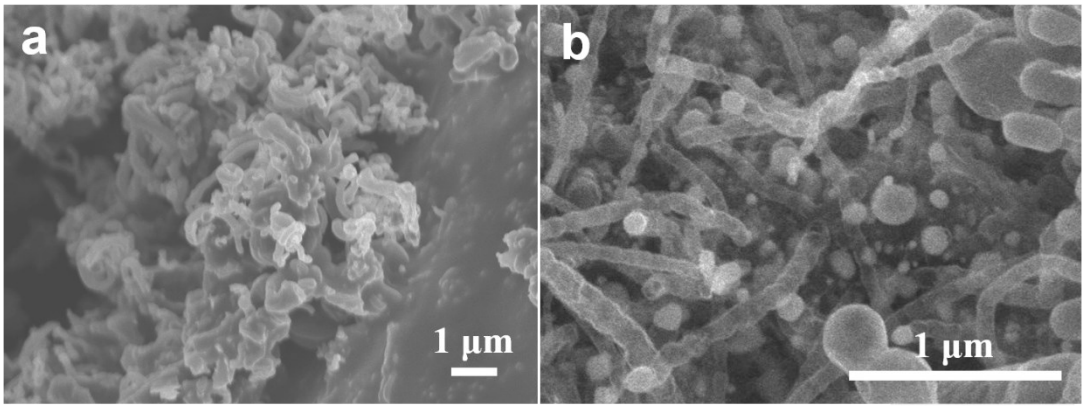

Fig. S4 SEM images of (a) Co_2P@NPCNTs-800 and (b) Co_2P@NPCNTs-1000.

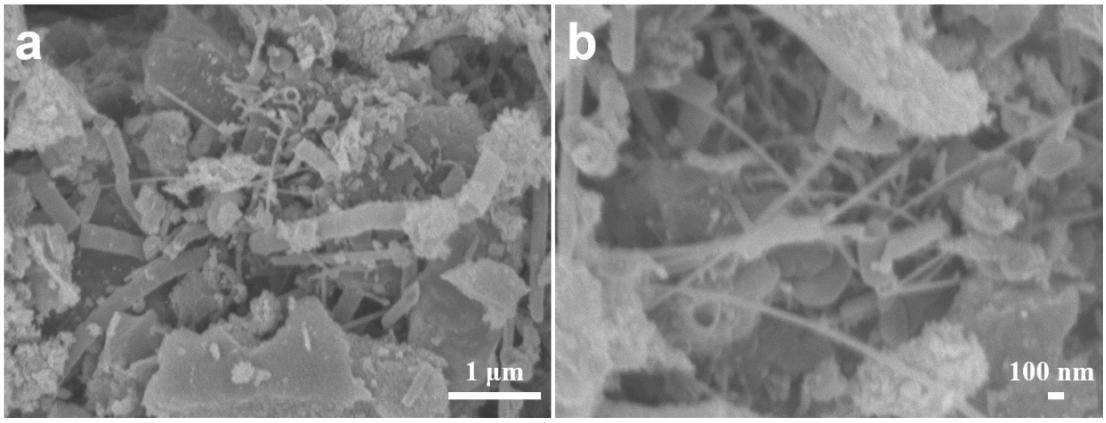

Fig. S5 (a) Low and (b) high-resolution SEM images of Co_2P@NPCNTs-1.

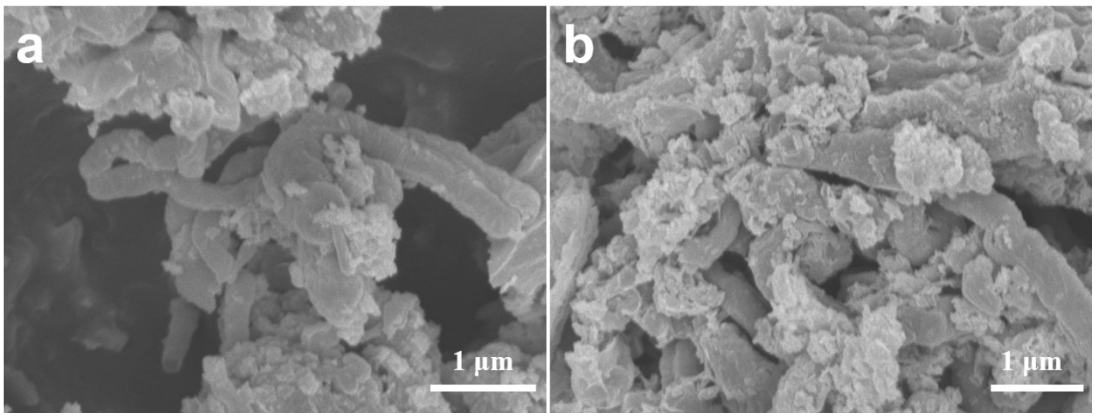

Fig. S6 (a) Low and (b) high-resolution SEM images of Co_2P@NPCNTs-3.

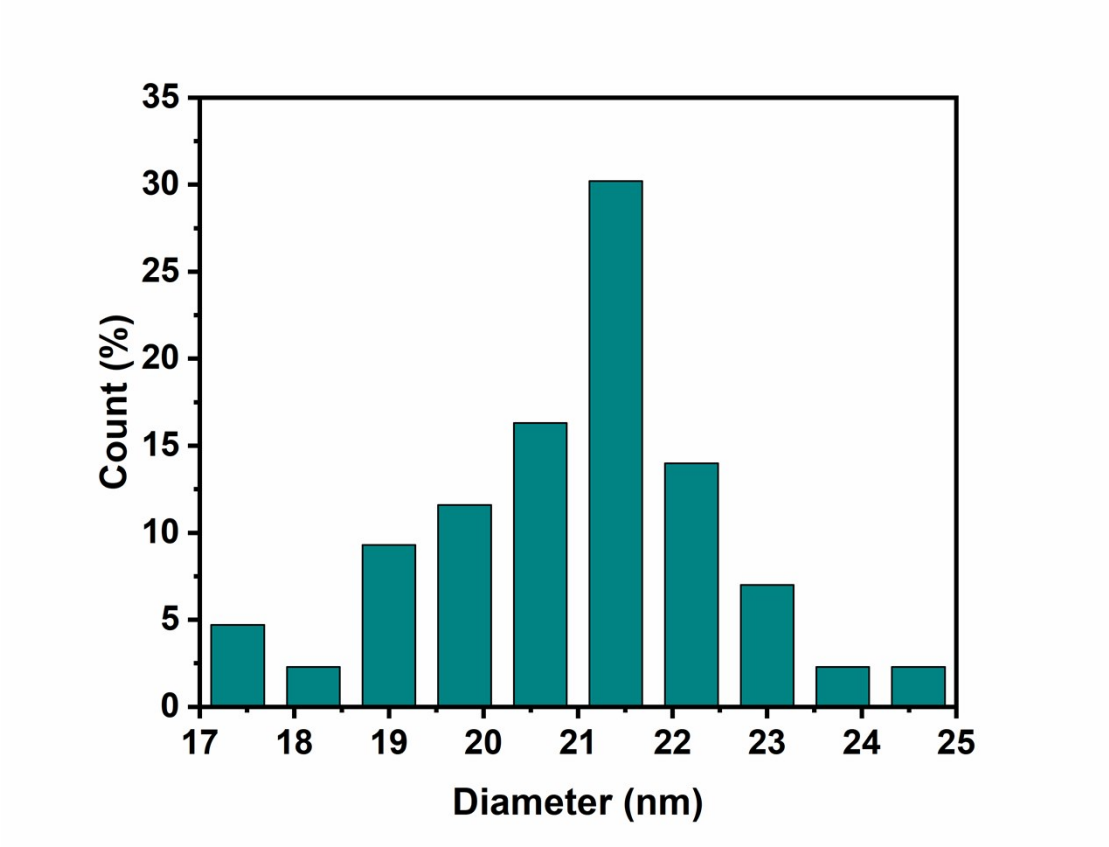

Fig. S7 Particle size distribution of Co_2P nanoparticles in Co_2P@NPCNTs-900.

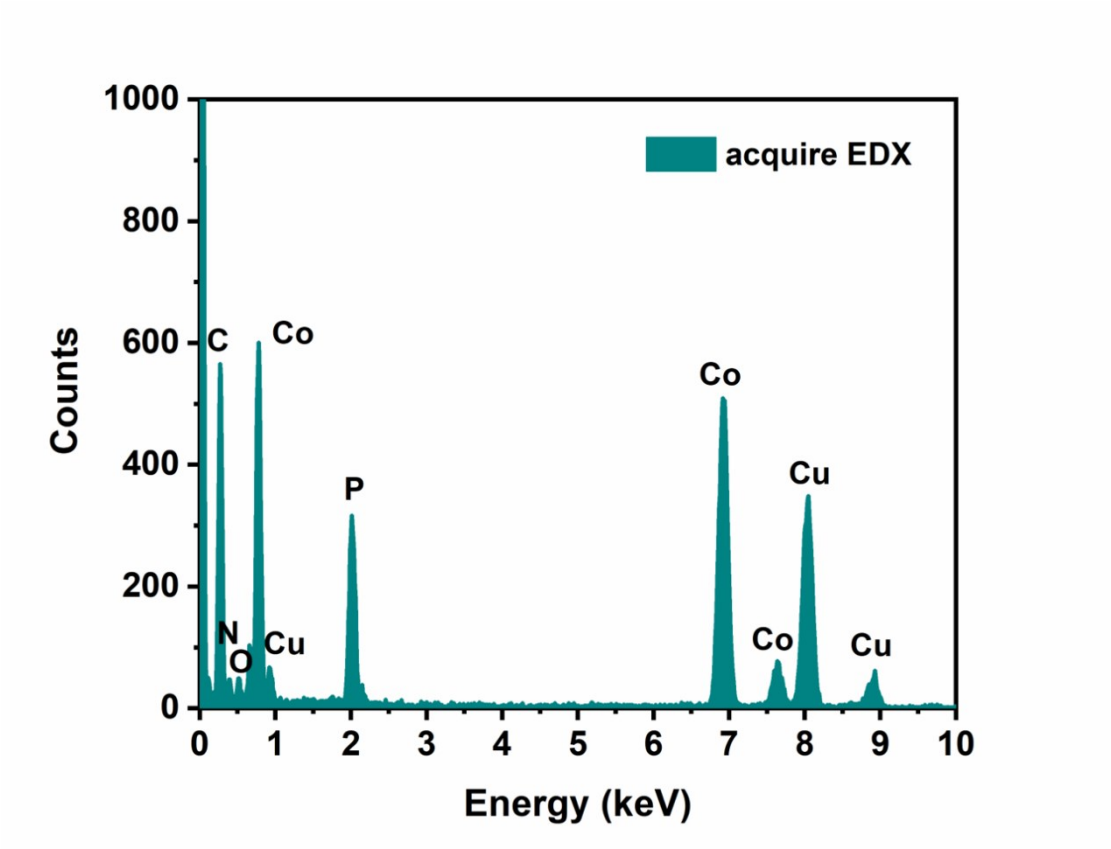

Fig. S8 Energy-dispersive spectrometer (EDS) of Co_2P@NPCNTs-900.

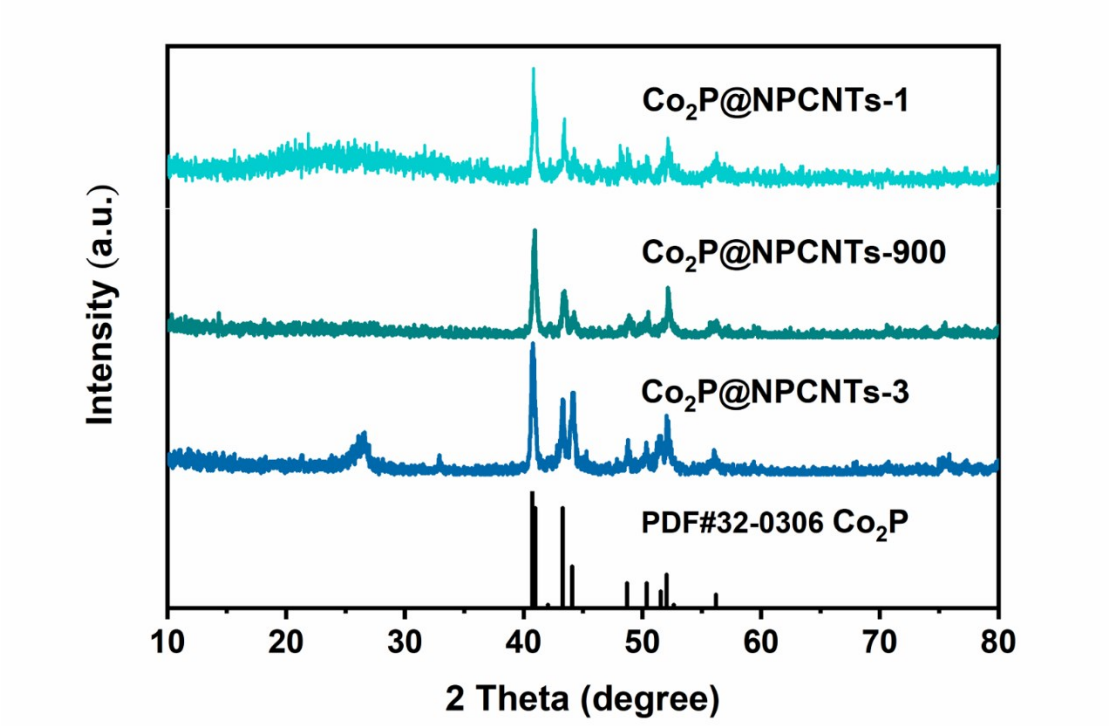

Fig. S9 XRD patterns of Co_2P@NPCNTs-1, Co_2P@NPCNTs-900 and Co_2P@NPCNTs-3.

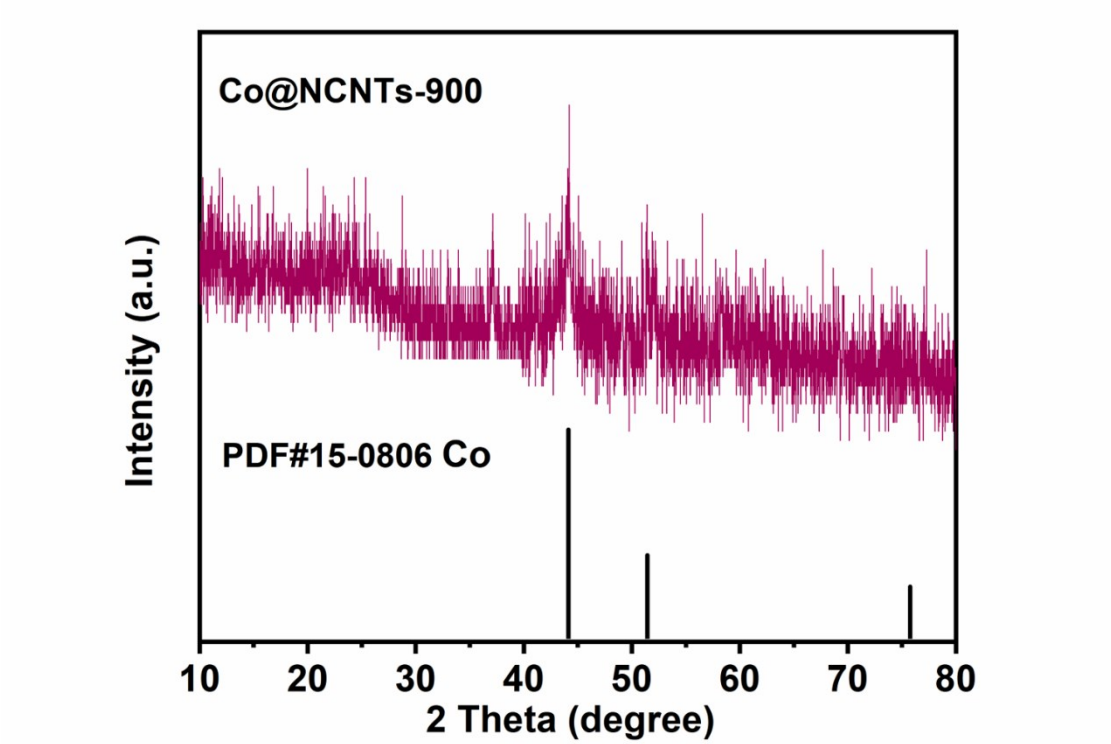

Fig. S10 XRD patterns of Co@NCNTs-900.

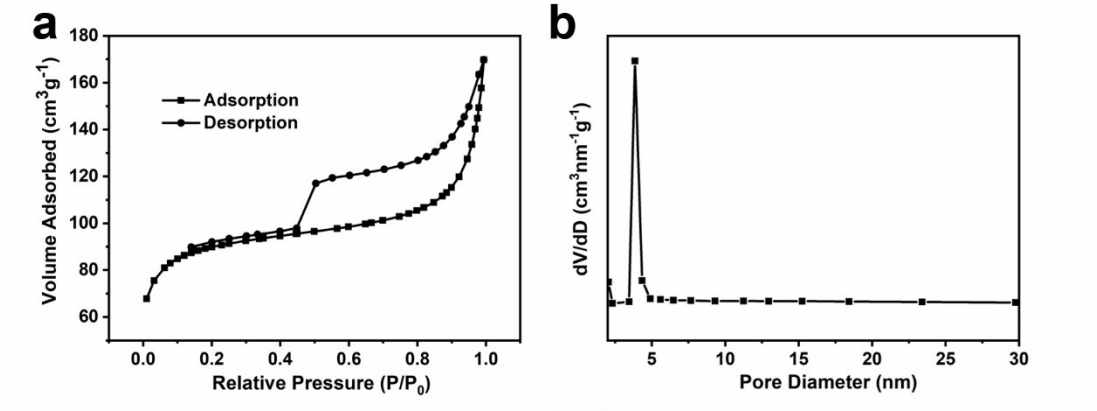

Fig. S11 (a) N_2 adsorption-desorption isotherms and (a) pore size distribution of Co_2P@NPCNTs-900.

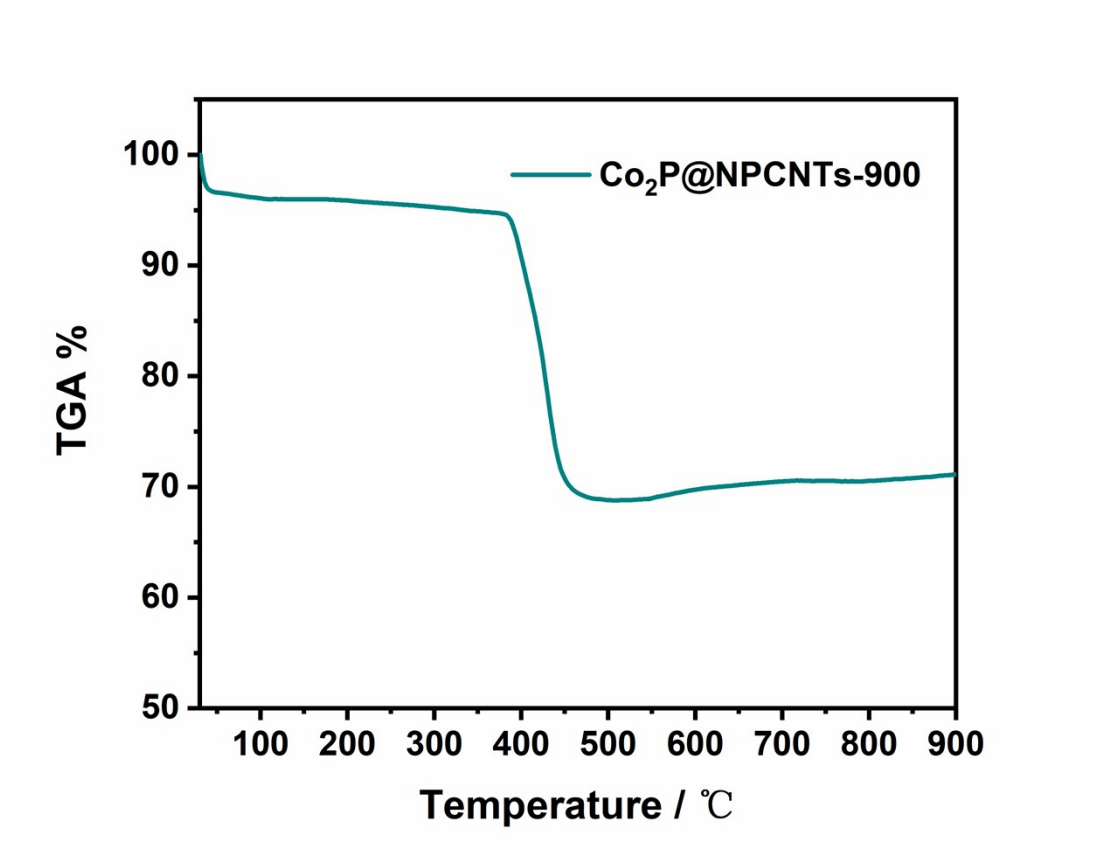

Fig. S12 TG curve of Co_2P@NPCNTs-900.

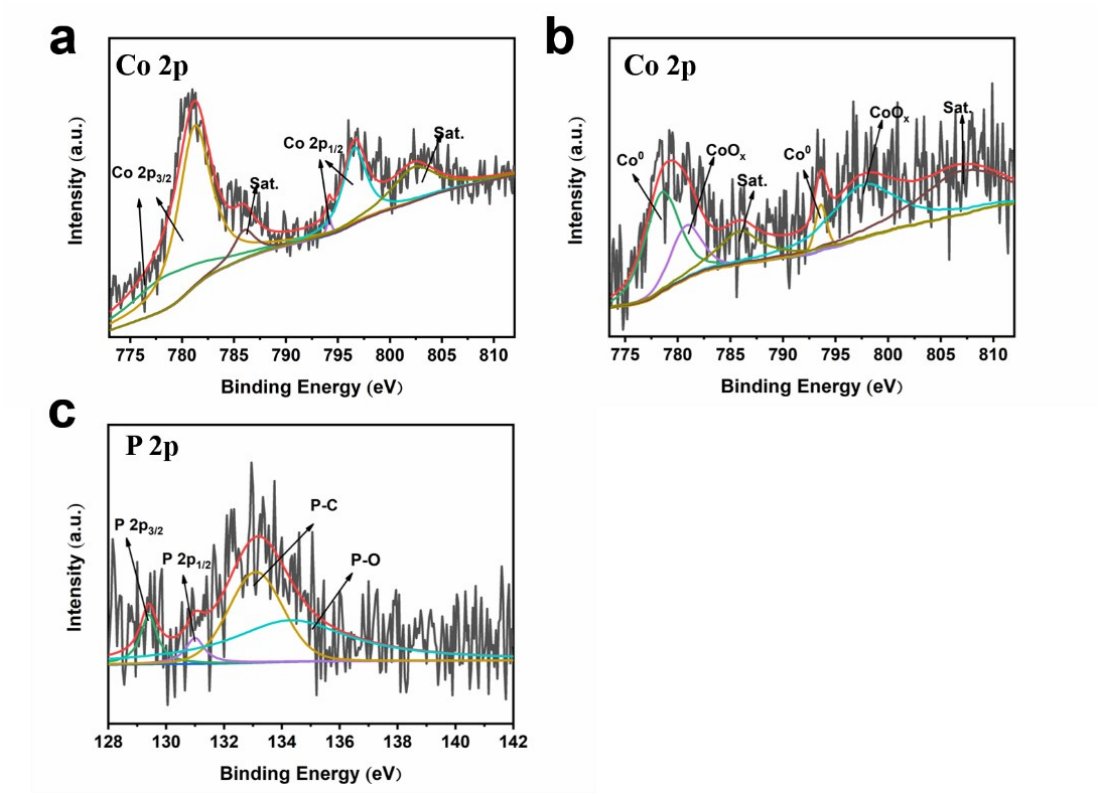

Fig. S13 High-resolution Co 2p XPS spectrum of Co_2P@NPC-900. (b) High-resolution Co 2p XPS spectrum of Co@NCNTs-900. (c) High-resolution P 2p XPS spectrum of Co_2P@NPC-900.

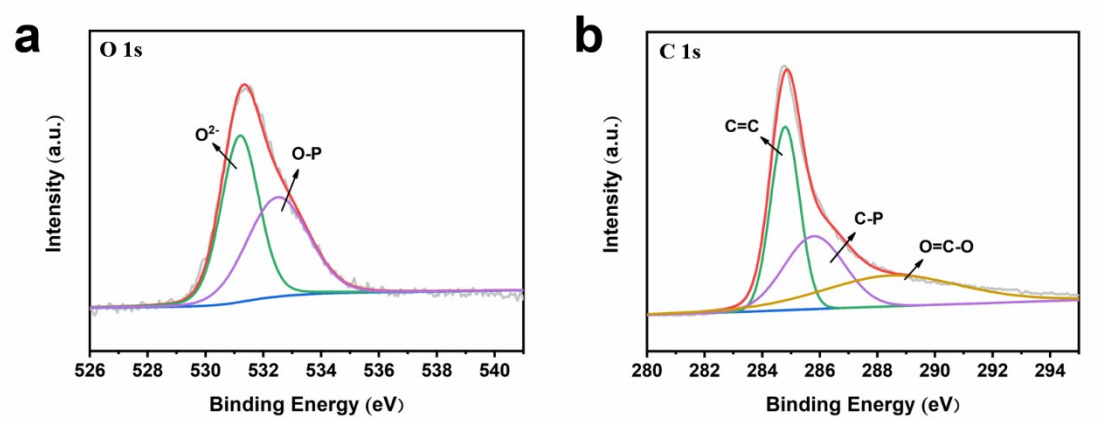

Fig. S14 High-resolution XPS spectra of O 1 (a) and C 1s (b) of Co_2P@NPCNTs-900.

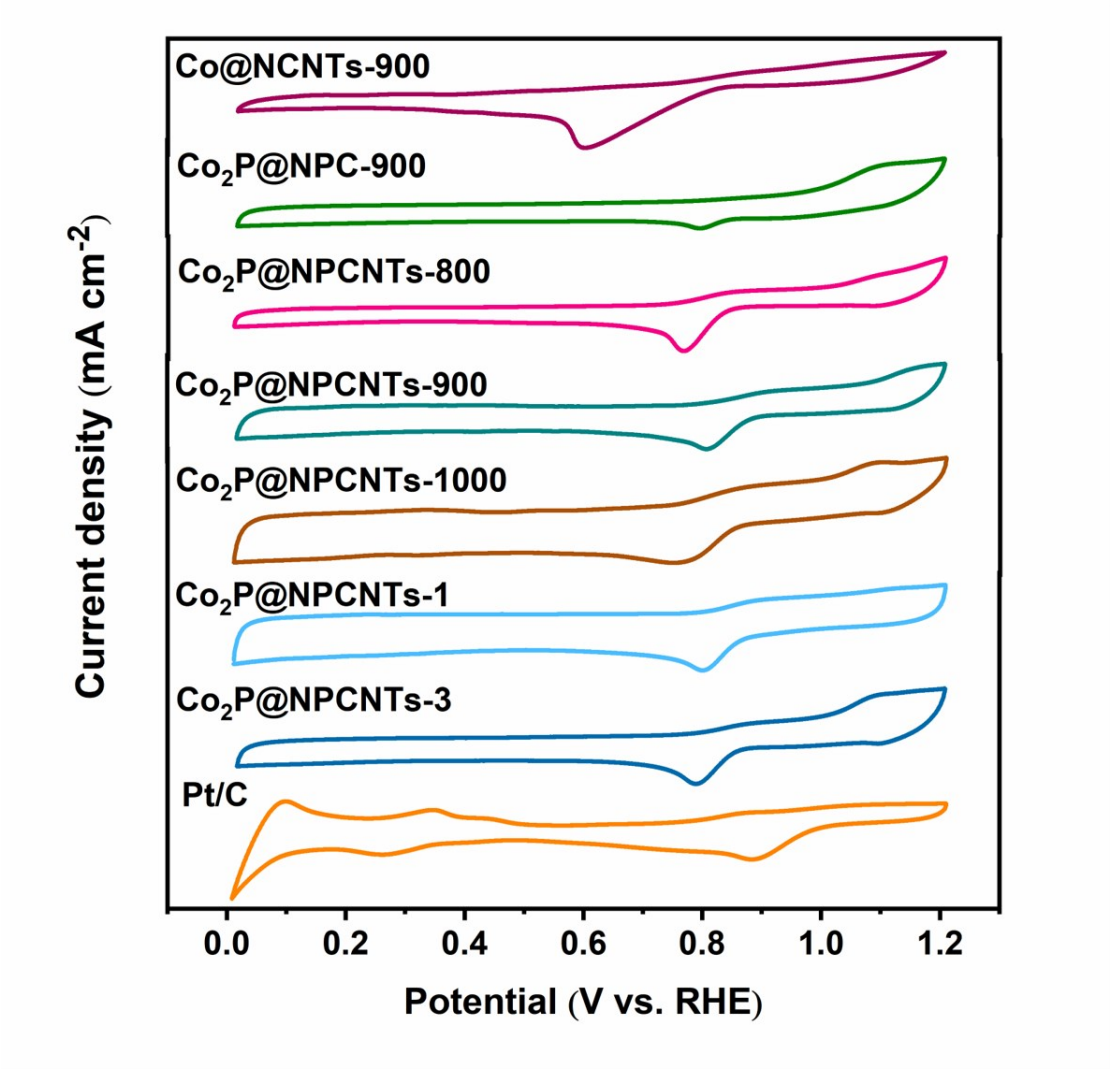

Fig. S15 CV curve of various samples in O_2-saturated 0.1 M KOH solution.

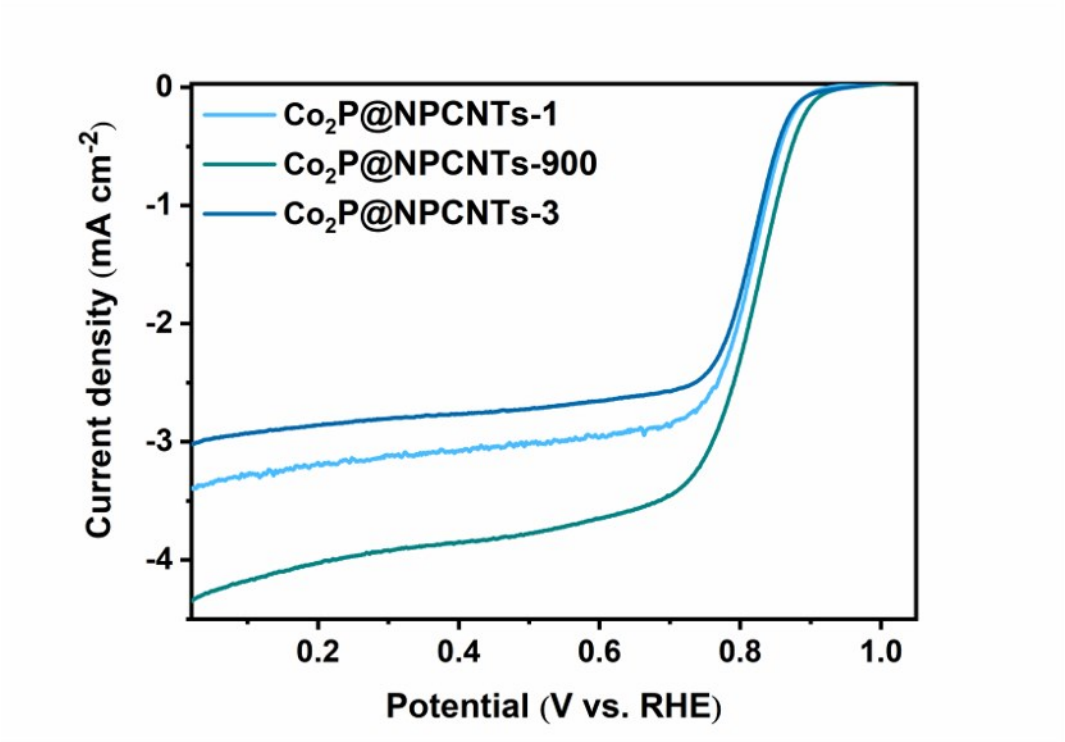

Fig. S16 ORR LSV curves of Co_2P@NPCNTs-1, Co_2P@NPCNTs-900 and Co_2P@NPCNTs-3.

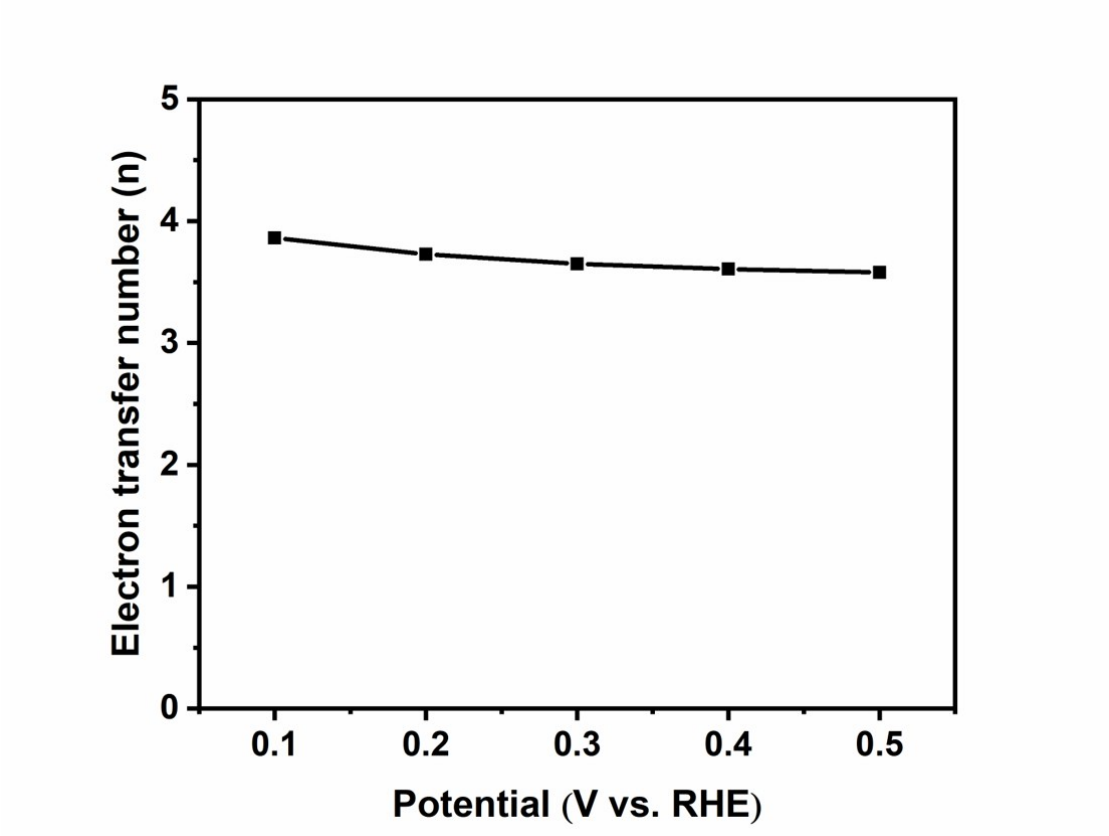

Fig. S17 The electron transfer number obtained from RDE results of Co_2P@NPCNTs-900.

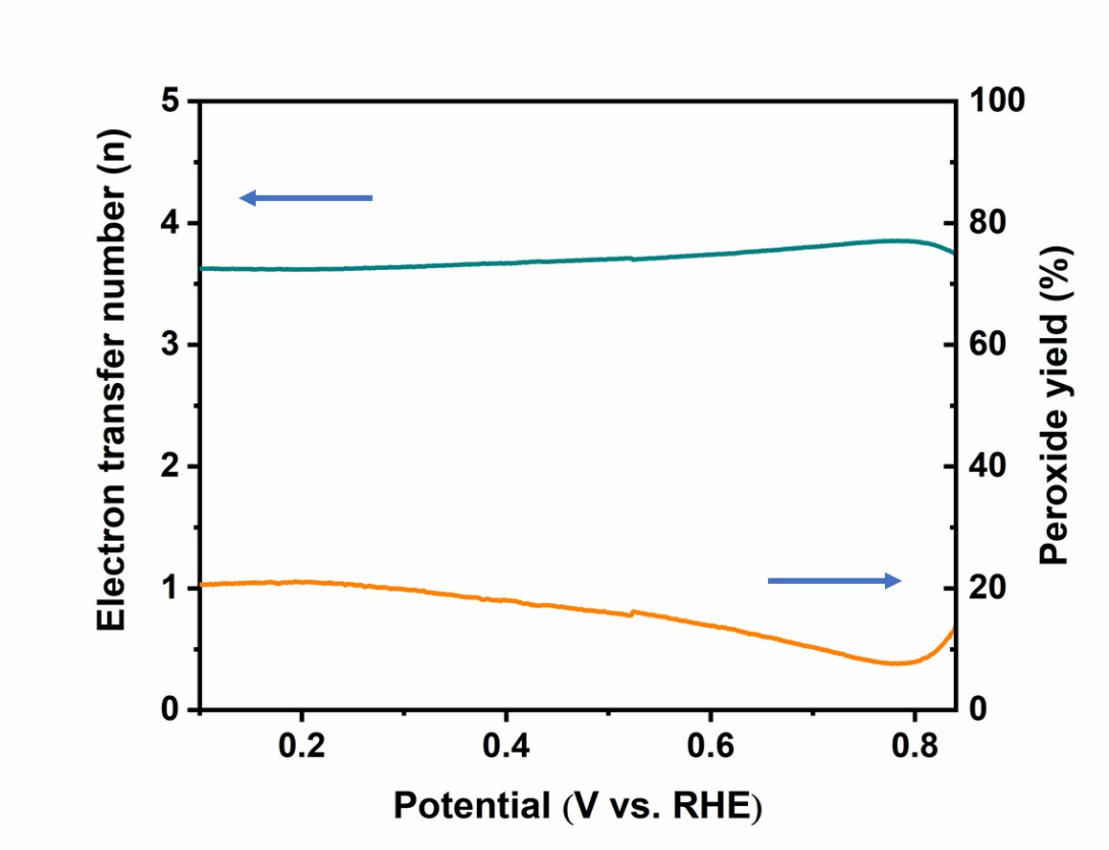

Fig. S18 Electron transfer number and H_2O_2 yield based on RRDE measurements.

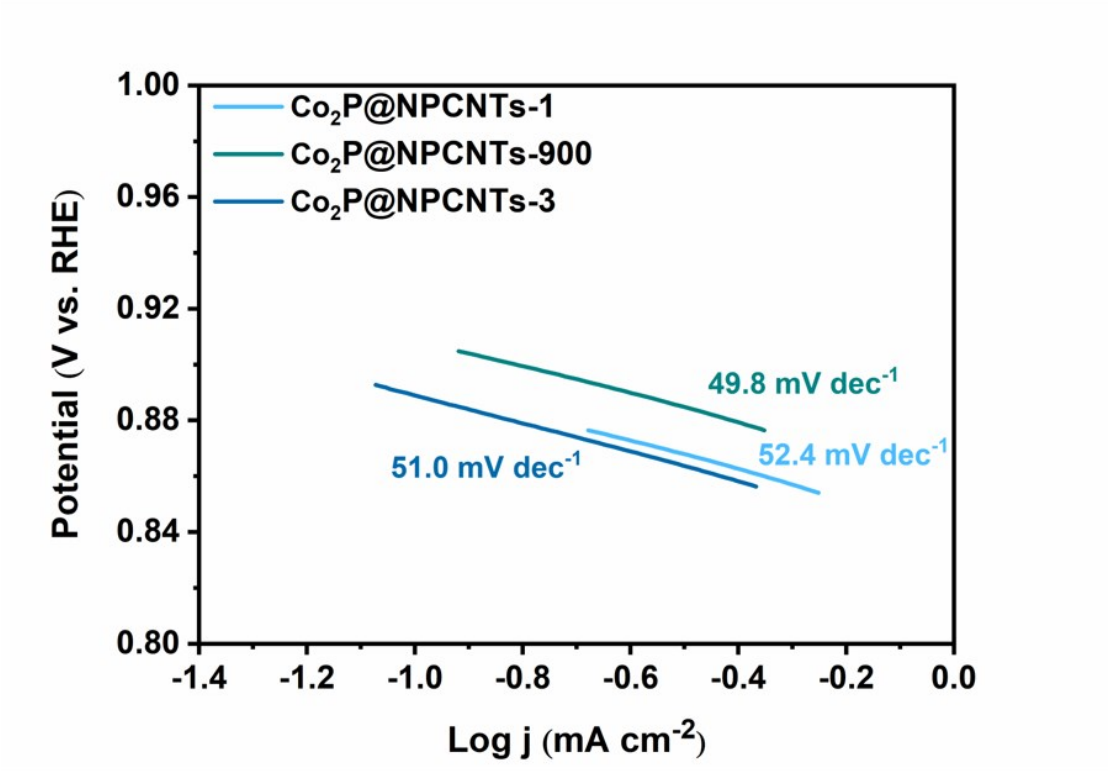

Fig. S19 The ORR Tafel plots of Co_2P@NPCNTs-1, Co_2P@NPCNTs-900 and Co_2P@NPCNTs-3.

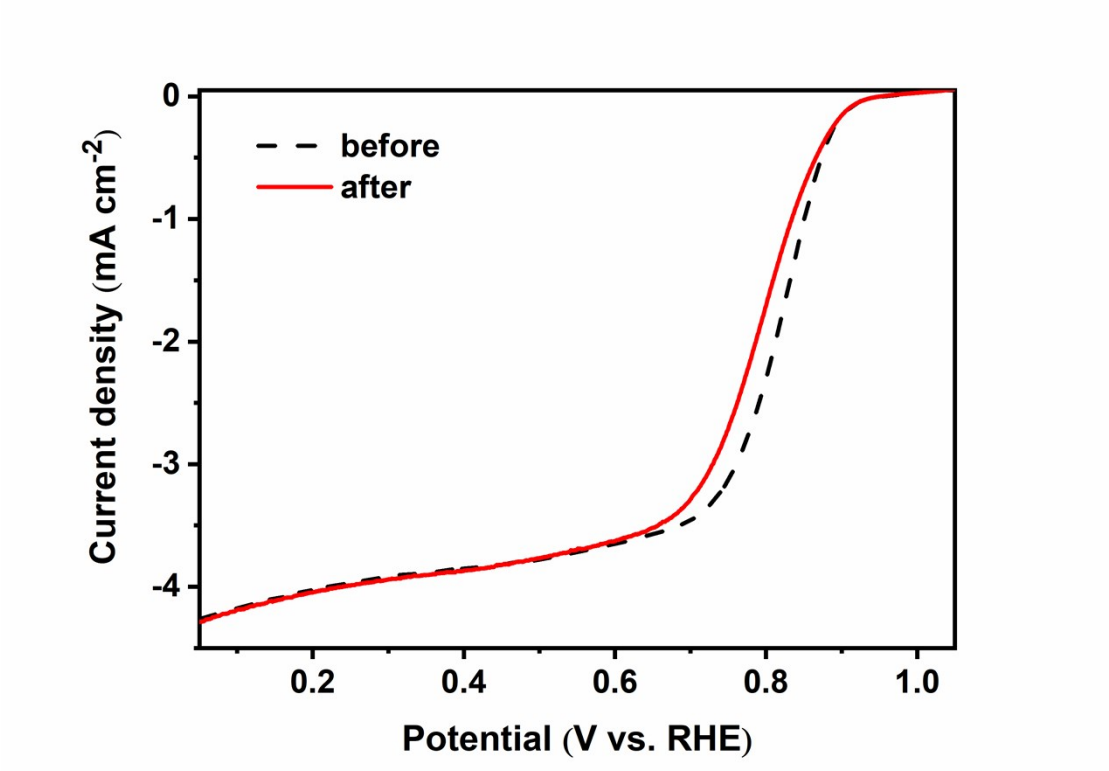

Fig. S20 ORR LSV curves of Co_2P@NPCNTs-900 before and after a continuous 5000-cycle CV scans.

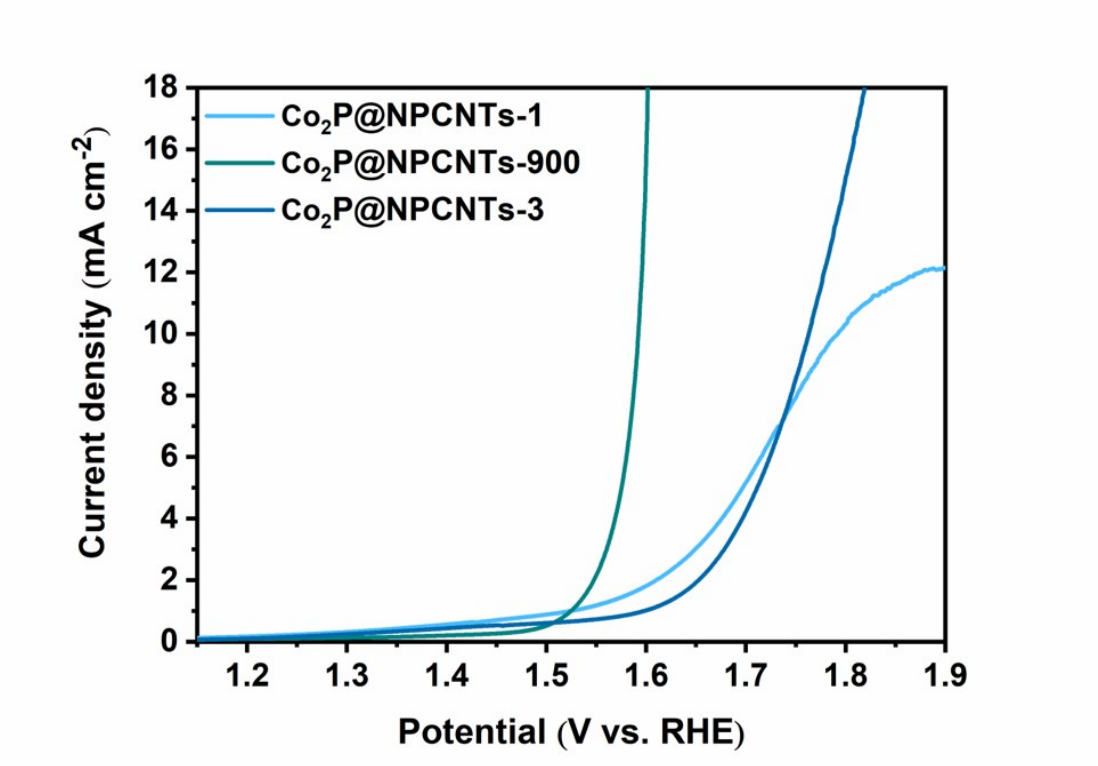

Fig. S21 OER LSV curves of Co_2P@NPCNTs-1, Co_2P@NPCNTs-900 and Co_2P@NPCNTs-3.

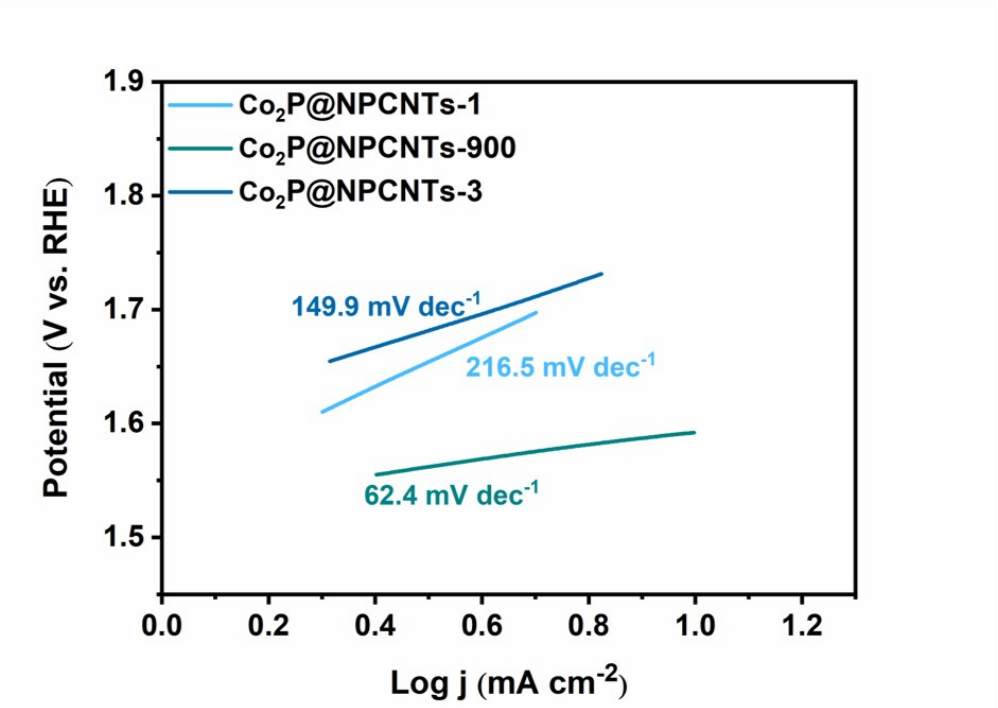

Fig. S22 The OER Tafel plots of Co_2P@NPCNTs-1, Co_2P@NPCNTs-900 and Co_2P@NPCNTs-3.

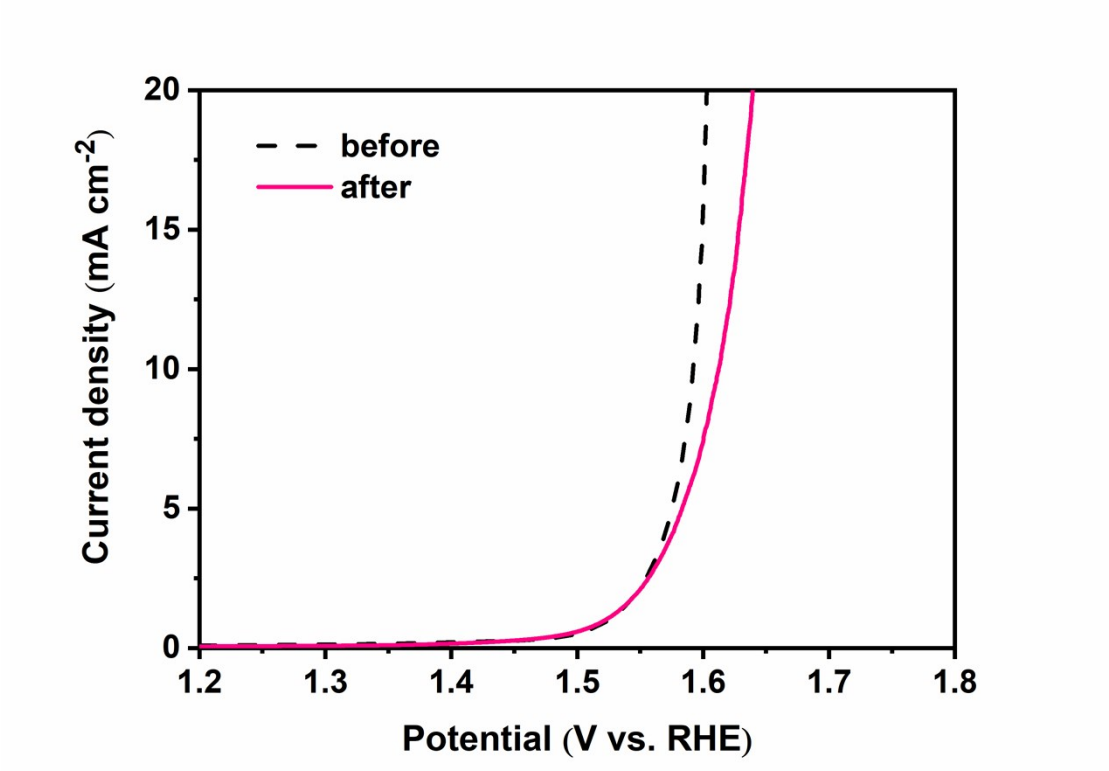

Fig. S23 OER LSV curves of Co_2P@NPCNTs-900 before and after a continuous 5000-cycle CV scans.

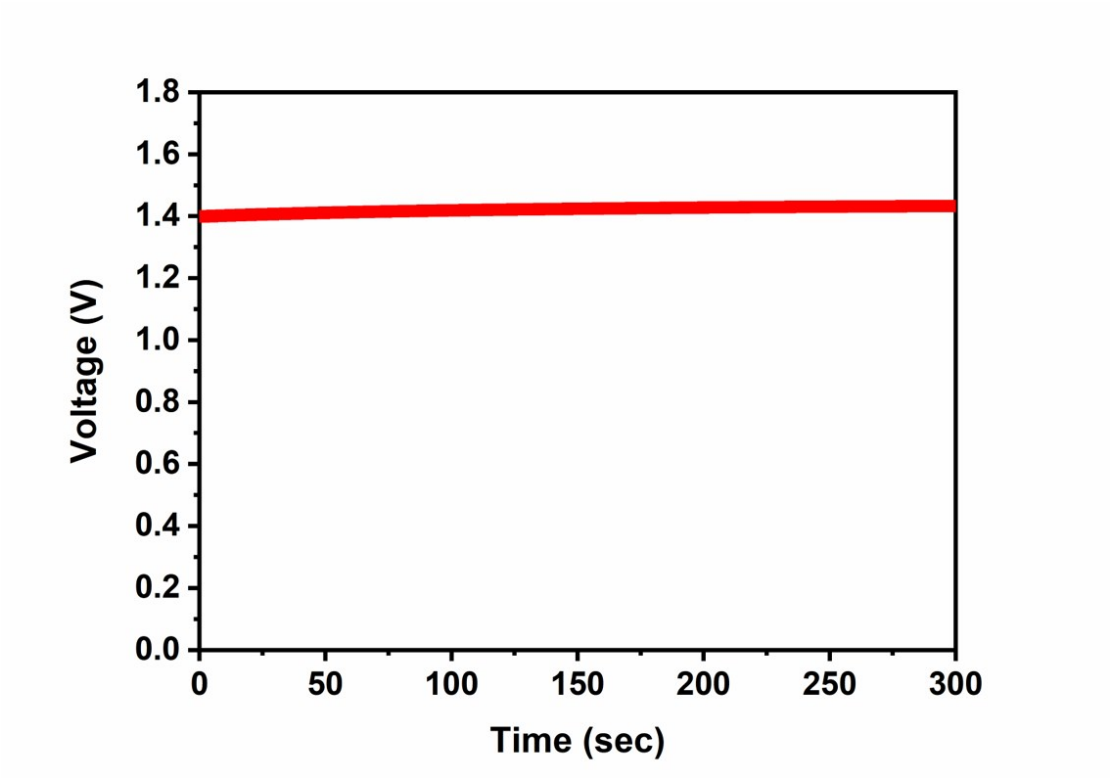

Fig. S24 Open-circuit plots of assembled rechargeable ZABs of Pt/C-RuO_2 catalysts.

Table S1 Elemental contents of C, O, N, P and Co in the Co_2P@NPCNTs-900 determined by XPS analysis.

Catalyst	C (at%)	P(at%)	N (at%)	O (at%)	Co (at%)
Co_2P@NPCNTs-900	77.99	2.63	10.40	7.25	1.72

Table S2. A survey of the catalytic performance of various electrocatalysts.

Catalysts	ORR		OER	Reference
	E_{onset} (V)	$E_{1/2}$ (V)	E_{10} (V)	
Co_2P@NPCNTs	0.94	0.80	1.59	**This work**
CoP@SNC	--	--	1.58	**Nanoscale** 2018, 10, 14613
N-GCNT/FeCo	1.03	0.92	1.73	**Adv. Energy Mater.** 2017, 7, 1602420
CoFe/N-GCT	0.91	0.79	1.67	**Angew. Chem. Int. Ed.** 2018, 130, 16398
Co-N-CNTs	0.97	0.90	1.69	**Adv. Funct. Mater.** 2018, 28, 1705048
Co_2P/CoN-in-NCNTs	0.96	0.85	1.65	**Adv. Funct. Mater.** 2018, 28, 1805641
Co_3O_4/NPGC	0.97	0.84	1.68	**Angew. Chem. Int. Ed.** 2016, 55, 4977
CoS_x@PCN/rGO	--	0.78	1.57	**Adv. Energy Mater.** 2018, 8, 1701642